

**Novel Coordination Isomerization in Organotin(IV) Compounds. Synthesis, Molecular Structures, and NMR Studies of  $\text{LSnPhX}_2$  ( $\text{X} = \text{Ph, Cl, Br, I, SPh}$ ),  $\text{LCH}_2\text{SnPhX}_2$  ( $\text{X} = \text{Ph, Cl, Br, I}$ ), and  $\text{LSiPh}_3$ , Where  $\text{LH}$  Is  $(2\text{-MeO-3-}^t\text{Bu-5-Me-C}_6\text{H}_2)_2\text{CH}_2$**

Dainis Dakternieks,\* Klaus Jurkschat\*,† and Ramon Tozer

*School of Biological and Chemical Sciences, Deakin University, Geelong 3217, Australia*

James Hook

*NMR Facility, University of New South Wales, Sydney 2052, Australia*

Edward R. T. Tiekink

*Department of Chemistry, University of Adelaide, South Australia 5005, Australia*

Received November 12, 1996<sup>⊗</sup>

The series of complexes  $\text{LSnPhX}_2$  (**1**,  $\text{X} = \text{Ph}$ ; **3**,  $\text{X} = \text{Cl}$ ; **4**,  $\text{X} = \text{Br}$ ; **5**,  $\text{X} = \text{I}$ ; **6**,  $\text{X} = \text{SPh}$ ),  $\text{LSiPh}_3$  (**2**),  $\text{LSnCl}_3$  (**7**),  $\text{LCH}_2\text{SnPhX}_2$  (**9**,  $\text{X} = \text{Ph}$ ; **10**,  $\text{X} = \text{Cl}$ ; **11**,  $\text{X} = \text{Br}$ ; **12**,  $\text{X} = \text{I}$ ) and  $\text{LCH}_2\text{SnCl}_3$  (**13**), where  $\text{LH}$  is bis(2-methoxy-3-*tert*-butyl-5-methylphenyl)methane (2-MeO-3-*t*-Bu-5-Me-C<sub>6</sub>H<sub>2</sub>)<sub>2</sub>CH<sub>2</sub>, has been synthesised, and compounds **1–6** have been characterized in the solid state by X-ray crystallography. Distorted tetrahedral geometries are found in the structures of **1** and **2**. By contrast, distorted trigonal bipyramidal geometries are found in the structures of **3–6**, owing to the presence of significant intramolecular Sn···O interactions that lie in the range from 2.559(4) Å for **3** to 2.989(4) Å for **6**; the magnitudes of the Sn···O interactions have been correlated with the Lewis acidity of the tin atoms in the  $\text{PhSnX}_2$  entities. NMR spectroscopy indicates a similar correlation in solution. Compounds **1**, **2**, **6**, and **9** are essentially four coordinate in solution between 30 and –100 °C. In compound **4**, intramolecular coordination of one of the methoxy groups results in the novel situation where both four- and five-coordinate tin species exist simultaneously at low temperature. At higher temperature, an average of these two coordination states is observed. The remaining compounds also participate in intramolecular exchange equilibria, with the position of the equilibrium being affected by both the Lewis acidity at tin and by the ring size; the six-membered rings in **10–13** are more labile than the five-membered rings in **3–5** and **7**. Adduct formation between tributylphosphine oxide,  $\text{Bu}_3\text{PO}$ , and compounds **3–5** is described.

### Introduction

Hydrolysis reactions of organotin(IV) halides have been established as viable sources of oligomeric tin clusters.<sup>1</sup> Factors that determine the pathways of such reactions are not yet fully understood, and consequently, reaction products have been somewhat unpredictable. For example, the partial hydrolysis of  $^i\text{PrSnCl}_3$  leads to a variety of products including  $^i\text{PrSn}(\text{OH})\text{Cl}_2 \cdot \text{H}_2\text{O}$ ,<sup>2</sup>  $(^i\text{PrSn})_9\text{O}_8(\text{OH})_6\text{Cl}_5 \cdot \text{DMSO}$ ,<sup>3</sup> and  $[(^i\text{PrSn})_{12}\text{O}_{14}(\text{OH})_6]^{2+}$ .<sup>4</sup> Hydrolysis of  $^n\text{BuSnCl}_3$ <sup>5</sup> or of  $^n\text{BuSn}(\text{O}^i\text{Pr})_3$ <sup>6</sup> leads to  $[(\text{BuSn})_{12}\text{O}_{14}(\text{OH})_6]^{2+}$ . Research to date has lacked a synthetic strategy aimed at controlling the oligomer

formation process. Given that tin–oxygen oligomers of predetermined size may have use in industrial applications,<sup>7</sup> the rational synthesis of such species remains an important synthetic target.

In an attempt to develop such designer molecular technology, we are interested in the effects of intramolecular donors on the hydrolysis pathways of mono- and diorganotin(IV) halides. Intramolecular donors may allow specific control over the geometry of tin sites from which additional linkages can form during hydrolysis. Accordingly, the study of intramolecular donor atom → Sn interactions has attracted some recent attention. Notably, the work of Willem *et al.*<sup>8</sup> has explored the nature of intramolecular O → Sn interactions versus

† Present address: Fachbereich Chemie der Universität, Lehrstuhl für Anorganische Chemie II, D-44221 Dortmund, Germany.

<sup>⊗</sup> Abstract published in *Advance ACS Abstracts*, July 1, 1997.

(1) *Chemistry of Tin*; Harrison, P. G., Ed.; Blackie: London, 1989; Chapter 2.

(2) Puff, H.; Reuter, H. *J. Organomet. Chem.* **1989**, *364*, 57.

(3) Puff, H.; Reuter, H. *J. Organomet. Chem.* **1989**, *368*, 173.

(4) Puff, H.; Reuter, H. *J. Organomet. Chem.* **1989**, *373*, 173.

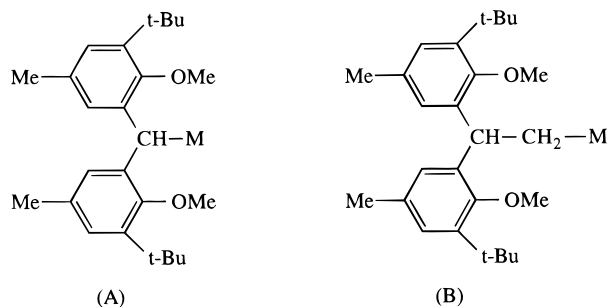
(5) Dakternieks, D.; Zhu, H.; Colton, R.; Tiekink, E. R. T. *J. Organomet. Chem.* **1994**, *476*, 33.

(6) Ribot, F. B. F.; Toledano, P.; Maquet, J.; Sanchez, C. *Inorg. Chem.* **1995**, *34*, 6371.

(7) Pinnavaia, T. J. *Science* **1983**, *220*, 4595.

(8) (a) Willem, R.; Delmotte, A.; De Borger, I.; Biesemans, M.; Gielen, M.; Kayser, F.; Tiekink, E. R. T. *J. Organomet. Chem.* **1994**, *480*, 255. (b) Kayser, F.; Biesemans, M.; Delmotte, A.; Verbruggen, I.; De Borger, I.; Gielen, M.; Willem, R.; Tiekink, E. R. T. *Organometallics* **1994**, *13*, 4026. (c) Fu, F.; Li, H.; Zhu, D.; Fang, Q.; Pan, H.; Tiekink, E. R. T.; Kayser, F.; Biesemans, M.; Verbruggen, I.; Willem, R.; Gielen, M. *J. Organomet. Chem.* **1995**, *490*, 163. (d) Biesemans, M.; Willem, R.; Damoun, S.; Geerlings, P.; Lahcini, M.; Jaumier, P.; Jousseau, B. *Organometallics* **1996**, *15*, 2237.

Lewis acidity of the organotin center, exploiting X-ray crystallographic as well as solid and solution state NMR methods. In this context, we now report on the synthesis and characterization of the polyfunctional ligand systems LH, bis(2-methoxy-3-*tert*-butyl-5-methylphenyl)methane [(2-MeO-3-*t*-Bu-5-Me-C<sub>6</sub>H<sub>2</sub>)<sub>2</sub>CH<sub>2</sub>], and LCH<sub>2</sub>-Br, as well as the series of compounds of type A and B.



- 1, M = SnPh<sub>3</sub>;      2, M = SiPh<sub>3</sub>  
 3, M = SnPhCl<sub>2</sub>;    4, M = SnPhBr<sub>2</sub>  
 5, M = SnPhI<sub>2</sub>;      6, M = SnPh(SPh)<sub>2</sub>  
 7, M = SnCl<sub>3</sub>
- 9, M = SnPh<sub>3</sub>;      10, M = SnPhCl<sub>2</sub>  
 11, M = SnPhBr<sub>2</sub>;    12, M = SnPhI<sub>2</sub>  
 13, M = SnCl<sub>3</sub>

These series were chosen because of their comparative ease of synthesis and because they contain two methoxy moieties capable of intramolecular coordination. The two ligands A and B allow study of the effect of moderation of the Lewis acidity of the tin center on the number and magnitude of the intramolecular tin-oxygen interactions. Furthermore, the series also permits comparison of the relative stability of five- and six-membered ring systems containing tin. Finally, this ligand design may eventually lead to octahedral tin compounds which have a facial arrangement of halides. Such an arrangement would give interesting polymeric hydrolysis products. X-ray crystal structure determinations of **1–6** are presented, as is a detailed NMR description of these compounds in solution. The hydrolysis reactions of these compounds will be the subject of a future paper.

## Experimental Section

**General Methods.** Solvents were dried by standard methods and distilled prior to use. All moisture- and air-sensitive reactions were performed under an argon atmosphere. Elemental analyses were carried out by the Microanalytical Laboratory of the Australian National University, Canberra. Solution NMR spectra were recorded on a JEOL GX 270 FT NMR spectrometer at 270.17 (<sup>1</sup>H), 67.84 (<sup>13</sup>C), 100.75 (<sup>119</sup>Sn), and 53.68 (<sup>29</sup>Si) MHz. Chemical shifts are relative to external Me<sub>4</sub>Si (<sup>1</sup>H, <sup>13</sup>C, <sup>29</sup>Si) and Me<sub>4</sub>Sn (<sup>119</sup>Sn). Spectra recorded in D<sub>2</sub>O were referenced against internal acetone at 2.1 (<sup>1</sup>H) and 30.3 (<sup>13</sup>C) ppm. 2-D correlation spectra were acquired from a heteronuclear correlation experiment using the standard JEOL pulse sequence VCHSHF. For <sup>119</sup>Sn–<sup>1</sup>H correlation, a delay of 5 ms was used. Correlation spectra were recorded with 2048 data points in F<sub>2</sub> and 128 increments in F<sub>1</sub> (64 scans per increment), using a relaxation delay of 1 s. The sample contained tris(acetylacetonato)chromium(III) as a paramagnetic relaxation agent. A shifted sinebell window function was applied in both dimensions. Solid state <sup>119</sup>Sn and <sup>13</sup>C NMR spectra were measured on a Bruker MSL-300S operating at 111.92 and 75.47 MHz, respectively. Samples of the LSnX<sub>3</sub> (ca. 110 mg) were packed into 4 mm double air-bearing zirconia rotors and spun at the magic angle at speeds up to 12 kHz. Spectra were usually obtained at ambient probe temperature (292 K) from single contact cross-

polarization (CP) experiments, except for those of the dibromide, **4**, and the diiodide, **5**, which were also measured at 330 K. The following CP conditions were used: Solid state <sup>119</sup>Sn NMR pulse width, 4.0 ms (90° pulse); contact time, 1.2 ms; recycle time, 10 s. Chemical shifts are reported with respect to tetracyclohexyltin (δ<sub>Sn</sub> –97.4 ppm), which was used to set up the CP conditions and as an external chemical shift standard. The isotropic peak, δ<sub>iso</sub>, in each spectrum was identified by comparing spectra acquired at various speeds. Acquisition of ca. 400–15000 scans was sufficient to obtain spectra with a satisfactory signal to noise ratio. Solid state <sup>13</sup>C NMR: pulse width, 4.0 ms (90° pulse <sup>1</sup>H pulse); contact time, 1 ms; recycle time 5 s. Chemical shifts are reported with respect to adamantane (δ<sub>C</sub> 37.8 ppm), which was used to set up the CP conditions. Spectra were acquired at various MAS speeds, usually 4–6 kHz, to distinguish signals from spinning side bands arising from the aromatic carbon signals. From 600–3000 scans were sufficient to obtain spectra with a satisfactory signal to noise ratio.

**Crystallography.** Intensity data for the colorless crystals were measured at room temperature (20 °C) on a Rigaku AFC6R diffractometer fitted with graphite-monochromatized Mo Kα radiation, λ = 0.710 73 Å. The ω:2θ scan technique (ω technique for **2** and **3**) was employed to measure data up to a maximum Bragg angle of 25.0° (27.5° for **1** and **6**). A 20% decrease in the net intensity values of three standard reflections measured after every 400 data acquisitions was noted for **4**, and the data set was corrected for this variation assuming a linear decrease. The data sets were corrected for Lorentz and polarization effects,<sup>9</sup> and an empirical absorption correction was applied in each case.<sup>10</sup> Relevant crystal data are given in Table 1.

The structures were solved by direct methods employing SHELXS86<sup>11</sup> for **1**, **2**, **4**, and **5** and SIR<sup>12</sup> for **3** and **6** and refined by a full-matrix least-squares procedure based on F<sup>2</sup>. Non-H atoms were refined with anisotropic displacement parameters, and H atoms were included in the models in their calculated positions (C–H 0.97 Å) with the following exceptions. In the refinements of **3** and **4**, disorder was noted for the C(13') *tert*-butyl group; the C(13a) and C(13b) atoms in **3** were refined isotropically, and for **4**, the methyl groups were modeled over five sites, two with 50% site occupancy and three with 67% site occupancy; these atoms were also refined isotropically. The refinements were continued until convergence employing σ weights; the analysis of variance showed no special features, indicating that an appropriate weighting scheme had been applied in each case. The absolute configuration of **6** was determined by reversing the signs of the reflections in each data set and comparing the refinements; final refinement details are given in Table 1. The numbering schemes employed are shown in Figures 1–4 (drawn with ORTEP<sup>13</sup> at 20, 25, 35, and 30% probability ellipsoids, respectively). The teXsan<sup>9</sup> package, installed on an Iris Indigo workstation, was employed for all calculations.

**Synthesis of Bis(2-methoxy-3-*tert*-butyl-5-methylphenyl)methane, LH.** To a 250 mL round bottom flask was added 25.0 g (73.4 mmol) of bis(2-hydroxy-3-*tert*-butyl-5-methylphenyl)methane (Tokyo Kasei), 22.33 g (0.16 mol) of anhydrous K<sub>2</sub>CO<sub>3</sub>, 150 mL of dry acetone, and 4 mL of a 10% KOH/methanol solution. The mixture was magnetically stirred, and Me<sub>2</sub>SO<sub>4</sub> (15.32 mL, 0.16 mol) was added dropwise, after which the mixture was heated at reflux for 18 h. The resulting solution

(9) teXsan: Structure Analysis Software; Molecular Structure Corporation: The Woodlands, Texas.

(10) Walker, N.; Stuart, D. *Acta Crystallogr., Sect. A* **1983**, *39*, 158.

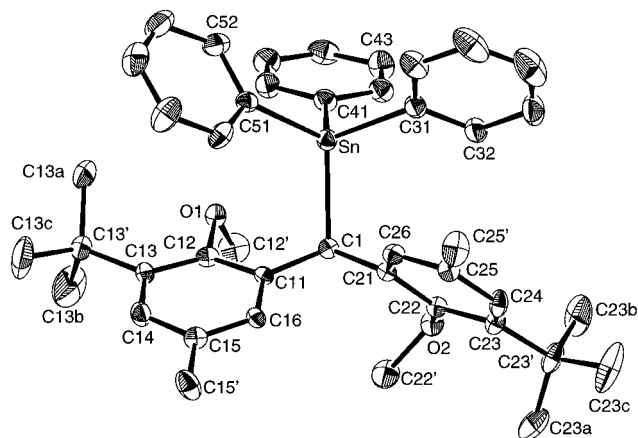
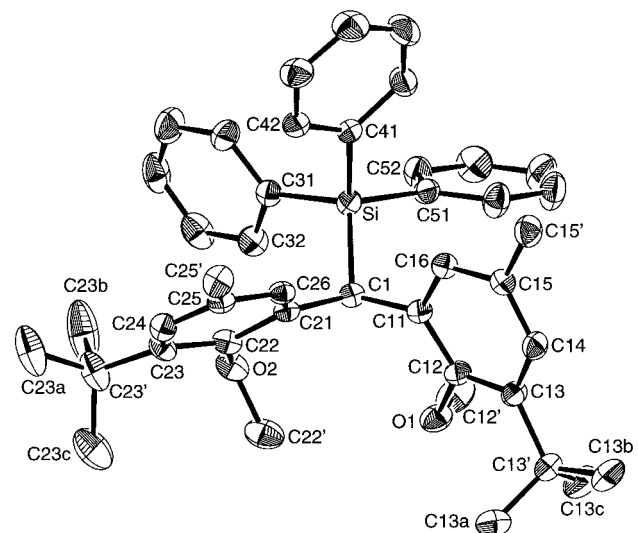
(11) Sheldrick, G. M. *SHELXS86, Program for the Automatic Solution of Crystal Structure*; University of Göttingen: Göttingen, Germany, 1986.

(12) Burla, M. C.; Camalli, M.; Cascarano, G.; Giacovazzo, C.; Polidori, G.; Spagna, R.; Viterbo, D. *J. Appl. Crystallogr.* **1989**, *22*, 389.

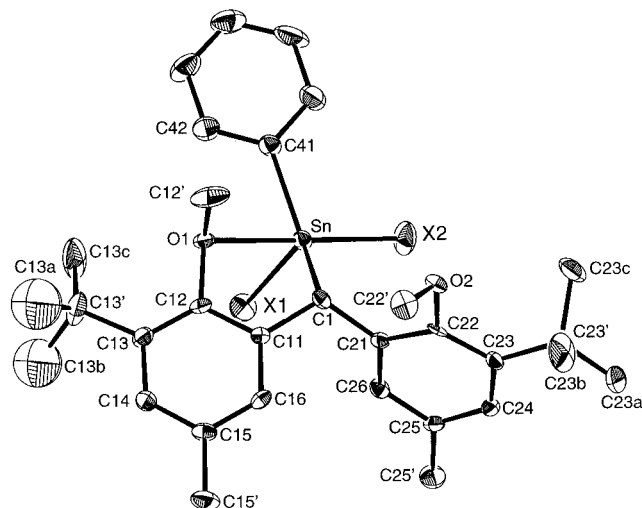
(13) Johnson, C. K. ORTEP. Report ORNL-5138; Oak Ridge National Laboratory: Oak Ridge, TN, 1976.

**Table 1. Crystallographic Data for 1–6**

	1	2	3	4	5	6
formula	C <sub>43</sub> H <sub>50</sub> O <sub>2</sub> Sn	C <sub>43</sub> H <sub>50</sub> O <sub>2</sub> Si	C <sub>31</sub> H <sub>40</sub> Cl <sub>2</sub> O <sub>2</sub> Sn	C <sub>31</sub> H <sub>40</sub> Br <sub>2</sub> O <sub>2</sub> Sn	C <sub>31</sub> H <sub>40</sub> I <sub>2</sub> O <sub>2</sub> Sn	C <sub>43</sub> H <sub>50</sub> O <sub>2</sub> S <sub>2</sub> Sn
fw	717.6	627.0	634.3	723.2	817.2	781.7
cryst size, mm	0.08 × 0.16 × 0.32	0.32 × 0.32 × 0.44	0.26 × 0.39 × 0.52	0.08 × 0.24 × 0.40	0.02 × 0.24 × 0.32	0.16 × 0.16 × 0.40
cryst syst	monoclinic	monoclinic	monoclinic	monoclinic	monoclinic	monoclinic
space group	<i>P</i> 2 <sub>1</sub> / <i>n</i>	<i>P</i> 2 <sub>1</sub> / <i>c</i>	<i>C</i> 2/ <i>c</i>	<i>P</i> 2 <sub>1</sub> / <i>c</i>	<i>P</i> 2 <sub>1</sub> / <i>c</i>	<i>P</i> 2/ <i>c</i>
<i>a</i> , Å	14.758(7)	14.793(6)	39.53(2)	21.305(9)	21.268(8)	19.757(7)
<i>b</i> , Å	16.000(5)	9.926(5)	10.103(6)	10.170(2)	10.127(8)	9.238(7)
<i>c</i> , Å	16.562(8)	25.549(8)	14.908(8)	15.312(6)	15.874(7)	22.768(4)
$\beta$ , deg	105.00(4)	91.38(3)	94.83(5)	107.26(3)	106.51(3)	102.86(2)
<i>V</i> , Å <sup>3</sup>	3777(2)	3750(2)	5931(6)	3168(1)	3278(5)	4051(3)
<i>Z</i>	4	4	8	4	4	4
$\rho_{\text{calcd}}$ , g cm <sup>-3</sup>	1.262	1.110	1.420	1.516	1.656	1.281
<i>F</i> (000)	1496	1352	2608	1448	1592	1624
$\mu$ , cm <sup>-1</sup>	7.09	0.96	10.67	33.60	26.87	7.66
transm factors	0.893–1.112	0.979–1.013	0.955–1.019	0.787–1.064	0.935–1.070	0.961–1.025
data colld	+ <i>h</i> , + <i>k</i> , $\pm$ <i>l</i>	+ <i>h</i> , + <i>k</i> , $\pm$ <i>l</i>	+ <i>h</i> , + <i>k</i> , $\pm$ <i>l</i>	$\pm$ <i>h</i> , + <i>k</i> , + <i>l</i>	$\pm$ <i>h</i> , + <i>k</i> , + <i>l</i>	+ <i>h</i> , + <i>k</i> , $\pm$ <i>l</i>
no. of data colld	9691	7334	7381	6197	6375	10214
$\theta_{\text{max}}$ , deg	27.5	25.0	25.0	25.0	25.0	27.5
no. of unique data	9345	7045	7274	5961	6144	9623
no. of unique data with $\geq 3.0\sigma(I)$	3458	3341	4391	2343	2607	5133
<i>R</i>	0.048	0.053	0.049	0.050	0.045	0.051
<i>R</i> <sub>w</sub>	0.041	0.053	0.057	0.046	0.042	0.050
residual density, e Å <sup>-3</sup>	0.38	0.31	1.52	1.05	0.60	1.36

**Figure 1.** Molecular structure and crystallographic numbering scheme for **1**.**Figure 2.** Molecular structure and crystallographic numbering scheme for **2**.

was filtered, the acetone filtrate was evaporated, and a pale yellow oil remained, which was dissolved in hexane and then placed in a freezer overnight. The solution was filtered again, and the filtrate was evaporated to yield 20.56 g (76%) of bis-(2-methoxy-3-*tert*-butyl-5-methylphenyl)methane (LH) as a pale yellow viscous oil, which was sufficiently pure to use in

**Figure 3.** Molecular structure and crystallographic numbering scheme for **3** (X = Cl), **4** (X = Br), and **5** (X = I).

further reactions. Passing a sample through a silica column (hexane eluent) gave an analytically pure sample, mp 230–232 °C. Anal. Calcd for C<sub>25</sub>H<sub>36</sub>O<sub>2</sub> (MW 368.59): C, 81.47; H, 9.84. Found: C, 81.05; H, 9.69. <sup>1</sup>H NMR (CDCl<sub>3</sub>):  $\delta$  1.39 (s, 18H, <sup>t</sup>Bu), 2.26 (s, 6H, Me), 3.72 (s, 6H, OMe), 4.06 (s, 2H, CH<sub>2</sub>), 6.74 (s, 2H, C<sub>6</sub>H<sub>2</sub>), 6.99 (s, 2H, C<sub>6</sub>H<sub>2</sub>). <sup>13</sup>C NMR (CDCl<sub>3</sub>):  $\delta$  21.0 (CH<sub>3</sub>), 30.3 (CH<sub>2</sub>), 31.0 (C(CH<sub>3</sub>)<sub>3</sub>), 34.8 (C(CH<sub>3</sub>)<sub>3</sub>), 61.2 (OCH<sub>3</sub>), C<sub>6</sub>H<sub>2</sub> (not assigned), 125.8, 129.7, 132.0, 133.8, 142.0, 156.2.

**Synthesis of Ph<sub>3</sub>SnL (1).** To a two-necked 250 mL round bottom flask was added 7.41 g (20.11 mmol) of LH and 80 mL of dry THF. The solution was cooled to –20 °C, and 8.38 mL of *n*-butyllithium (2.4 M) was added dropwise; the solution was stirred at this temperature for a further 2.5 h. The deep red mixture was cooled to –55 °C, followed by dropwise addition of a 20 mL solution of THF containing 7.75 g (20.11 mmol) Ph<sub>3</sub>SnCl. Just prior to the final addition of the Ph<sub>3</sub>SnCl solution, the now orange color faded to pale yellow. The sample was stirred overnight at ambient temperature, the THF was removed under vacuum, and 50 mL of diethyl ether was added. This solution was hydrolyzed with 20 mL of water, and the aqueous phase was washed with two 25 mL portions of diethyl ether; all extracts were combined and dried over anhydrous magnesium sulfate. The pale yellow solution was filtered. Evaporation of the solvent gave a white solid, which was dissolved in 150 mL of boiling hexane and cooled in a

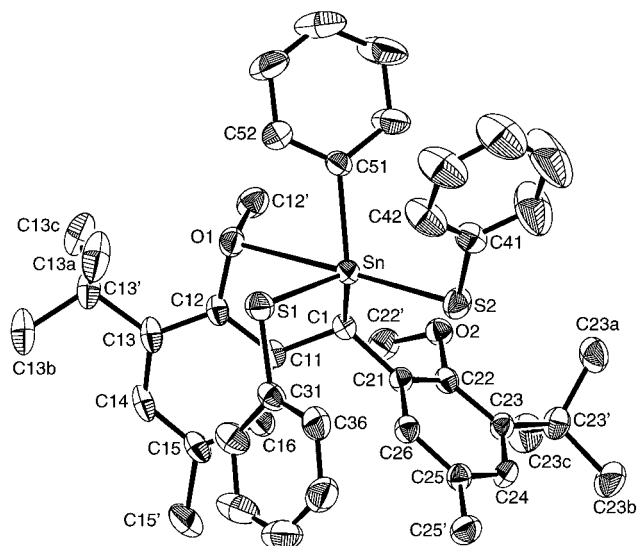


**Figure 4.** Molecular structure and crystallographic numbering scheme for **6**.

refrigerator overnight to give 13.7 g (95%) of **1** as a white crystalline solid, mp 187–190 °C. Anal. Calcd for  $C_{43}H_{50}O_2$ -Sn (MW 717.60): C, 71.98; H, 7.02. Found: C, 71.73; H, 6.97.  $^1H$  NMR ( $CDCl_3$ ):  $\delta$  1.28 (s, 18H,  $^tBu$ ), 2.02 (s, 6H, Me), 3.56 (s, 6H, OMe), 5.04 (s,  $^1H$ , CH,  $^2J(^{119}Sn-^1H) = 101$  Hz), 6.82 (2H,  $C_6H_2$ ), 7.0–7.77 (complex pattern, 17H,  $C_6H_2$ , SnPh $_3$ ).  $^{13}C$  NMR ( $CDCl_3$ ):  $\delta$  21.0 ( $CH_3$ ), 31.0 ( $C(CH_3)_3$ ), 33.4 (CH,  $^1J(^{119}Sn-^{13}C) = 380$  Hz), 34.7 ( $C(CH_3)_3$ ), 61.2 (OCH $_3$ ),  $C_6H_2$  (not assigned), 124.5, 130.1, 132.1, 135.2, 142.0, 155.1; Sn-Ph $_3$ : 141.2 ( $C_i$ ,  $^1J(^{119}Sn-^{13}C) = 481$  Hz), 136.7 ( $C_o$ ), 127.6 ( $C_m$ ), 127.8 ( $C_p$ ).

**Synthesis of Ph $_3$ SiL (2).** To a two-necked 250 mL round bottom flask was added 3.81 g (10.33 mmol) of LH and 60 mL of dry THF. The solution was cooled to –20 °C, 4.40 mL of *n*-butyllithium (2.35 M) was added dropwise, and the solution was stirred at this temperature for 2.5 h. The deep red mixture was cooled to –55 °C, followed by dropwise addition of a THF solution of Ph $_3$ SiCl (3.05 g, 10.33 mmol in 20 mL). The pale yellow solution was stirred overnight at ambient temperature, the THF was then removed under vacuum, and 50 mL of diethyl ether was added. This solution was hydrolyzed with 20 mL of water, and the aqueous phase was washed with two 25 mL portions of diethyl ether. The combined diethyl ether extracts were dried over anhydrous magnesium sulfate. Filtration and evaporation of the solution gave a white solid. The solid was dissolved in 50 mL of hot hexane, which upon cooling in a refrigerator overnight gave 4.67 g (72%) of **2** as a white crystalline solid, mp 193–195 °C. Anal. Calcd for  $C_{43}H_{50}O_2Si$  (MW 627.00): C, 82.38; H, 8.04. Found: C, 82.00; H, 7.89.  $^1H$  NMR ( $CDCl_3$ ):  $\delta$  1.29 (s, 18H,  $^tBu$ ), 2.10 (s, 6H, Me), 3.49 (s, 6H, OMe), 5.38 (s,  $^1H$ , CH), 6.92 (2H,  $C_6H_2$ ), 7.20–7.77 (complex pattern, 17H,  $C_6H_2$ , SiPh $_3$ ).  $^{13}C$  NMR ( $CDCl_3$ ):  $\delta$  21.2 ( $CH_3$ ), 26.4 (CH), 31.3 ( $C(CH_3)_3$ ), 35.1 ( $C(CH_3)_3$ ), 61.9 (OCH $_3$ ),  $C_6H_2$  (not assigned), 125.6, 130.7, 131.5, 134.7, 135.0, 155.4 ppm; SiPh $_3$ : 142.7 ( $C_i$ ), 137.0 ( $C_o$ ), 127.1 ( $C_m$ ), 129.0 ( $C_p$ ).  $^{29}Si$  NMR ( $CH_2Cl_2$ ):  $\delta$  –22.7.

**Synthesis of PhCl $_2$ SnL (3).** To a solution of **1** (4.0 g, 5.57 mmol) in 45 mL of acetone cooled to 0 °C was added, in small portions, 3.48 g of HgCl $_2$  (11.14 mmol). The solution was stirred at this temperature for 15 min, after which it was left to stir overnight at ambient temperature. The turbid liquid was then evaporated under vacuum, and 20 mL of  $CH_2Cl_2$  was added. This solution was placed in the freezer overnight and then filtered, and the volume was reduced to approximately 15 mL. The solution was placed in the freezer overnight, filtered again, and evaporated under vacuum to yield a colorless solid. Recrystallization from hexane afforded 3.1 g (88%) of **3**, mp 149–152 °C. Anal. Calcd for  $C_{31}H_{40}O_2SnCl_2$

(MW 634.29): C, 58.71; H, 6.36; Cl, 11.19. Found: C, 58.21; H, 6.51; Cl, 11.64.  $^1H$  NMR ( $CDCl_3$ ):  $\delta$  1.39 (s, 18H,  $^tBu$ ), 2.26 (s, 6H, Me), 3.50 (s, 6H, OMe), 4.64 (s,  $^1H$ , CH,  $^2J(^{119}Sn-^1H) = 128$  Hz), 6.79 (s, 2H,  $C_6H_2$ ), 7.10 (s, 2H,  $C_6H_2$ ), 7.3–8.0 (complex pattern, 5H, SnPh).  $^{13}C$  NMR ( $CDCl_3$ ):  $\delta$  21.2 ( $CH_3$ ), 31.8 ( $C(CH_3)_3$ ), 35.4 ( $C(CH_3)_3$ ), 44.5 (CH,  $^1J(^{119}Sn-^{13}C) = 673$  Hz), 64.7 (OCH $_3$ ),  $C_6H_2$  (not assigned), 128.7, 130.1, 130.7, 134.3, 142.4, 154.1; SnPh 142.9 ( $C_i$ ), 135.4 ( $C_o$ ), 129.9 ( $C_m$ ), 127.7 ( $C_p$ ).

**Synthesis of PhBr $_2$ SnL (4).** To a 25 mL toluene solution of **1** (1.0 g, 1.39 mmol) at –78 °C was added 0.446 g (2.78 mmol) of Br $_2$  in 10 mL of methanol. The solution was stirred at –78 °C for 25 min and then stirred for further 2 h at ambient temperature. The clear colorless solution was evaporated under vacuum to give a pale yellow solid, which was recrystallized from hexane to yield 0.76 g (75%) of **4** as a white solid, mp 134–136 °C. Anal. Calcd for  $C_{31}H_{40}O_2SnBr_2$  (MW 723.20): C, 51.49; H, 5.58; Br, 22.10. Found: C, 51.71; H, 5.85; Br, 22.24.  $^1H$  NMR ( $CDCl_3$ ):  $\delta$  1.41 (s, 18H,  $^tBu$ ), 2.26 (s, 6H, Me), 3.59 (s, 6H, OMe), 5.00 (s,  $^1H$ , CH,  $^1J(^{119}Sn-^1H) = 108$  Hz), 6.87 (s, 2H,  $C_6H_2$ ), 7.09 (s, 2H,  $C_6H_2$ ), 7.3–8.0 (complex pattern, 5H, SnPh).  $^{13}C$  NMR ( $CDCl_3$ ):  $\delta$  21.2 ( $CH_3$ ), 31.7 ( $C(CH_3)_3$ ), 35.4 ( $C(CH_3)_3$ ), 44.8 (CH,  $^1J(^{119}Sn-^{13}C) = 577$  Hz), 63.6 (OCH $_3$ ),  $C_6H_2$  (not assigned), 128.8, 130.3, 132.8, 133.7, 142.1, 154.7; SnPh 143.8 ( $C_i$ ),  $^1J(^{119}Sn-^{13}C) = 660$  Hz), 134.8 ( $C_o$ ), 129.9 ( $C_m$ ), 127.7 ( $C_p$ ).

**Synthesis of PhI $_2$ SnL (5).** To a 100 mL round bottom flask was added 50 mL of  $CH_2Cl_2$  and 3.0 g (4.18 mmol) of **1**; 2.12 g (8.36 mmol) of I $_2$  was then added in small portions over 1 h. The pale yellow solution was stirred overnight, then evaporated under vacuum to give a yellow oil. The oil was then dissolved in hexane and placed in the refrigerator overnight to yield 2.8 g (82%) of **5** as a pale yellow solid, mp 160–162 °C. Anal. Calcd for  $C_{31}H_{40}O_2SnI_2$  (MW 817.19): C, 45.57; H, 4.93; I, 31.06. Found: C, 45.62; H, 4.83; I, 31.44.  $^1H$  NMR ( $CDCl_3$ ):  $\delta$  1.43 (s, 18H,  $^tBu$ ), 2.28 (s, 6H, Me), 3.56 (s, 6H, OMe), 5.15 (s,  $^1H$ , CH,  $^1J(^{119}Sn-^1H) = 88$  Hz), 6.95 (s, 2H,  $C_6H_2$ ), 7.09 (s, 2H,  $C_6H_2$ ), 7.00–7.70 (complex pattern, 5H, SnPh).  $^{13}C$  NMR ( $CDCl_3$ ):  $\delta$  21.4 ( $CH_3$ ), 31.7 ( $C(CH_3)_3$ ), 35.2 ( $C(CH_3)_3$ ), 42.7 (CH,  $^1J(^{119}Sn-^{13}C) = 476$  Hz), 62.4 (OCH $_3$ ),  $C_6H_2$  (not assigned), 129.8, 130.5, 133.3, 133.9, 142.5, 155.3; SnPh 144.4 ( $C_i$ ,  $^1J(^{119}Sn-^{13}C) = 516$  Hz), 134.8 ( $C_o$ ), 128.9 ( $C_m$ ), 127.7 ( $C_p$ ).

**Synthesis of Ph(SPh) $_2$ SnL (6).** To 20 mL of dry MeOH was added 0.0474 g (2.06 mmol) of Na, the solution was stirred for 20 min, and 0.212 mL (2.06 mmol) of thiophenol was added dropwise. After a further 20 min of stirring, a solution of **4** (0.747 g, 1.03 mmol in 15 mL of  $CHCl_3$ ) was added dropwise and the resulting solution stirred overnight. The solvent was removed under vacuum, and the resulting clear oil was dissolved in hexane and placed in the refrigerator overnight to yield 0.653 g (81%) of **6** as a white solid, mp 131–133 °C.  $\delta(^{119}Sn$  MAS): 28 ppm. Anal. Calcd for  $C_{43}H_{50}O_2S_2Sn$  (MW 781.73): C, 66.07; H, 6.45. Found: C, 66.63; H, 6.69.  $^1H$  NMR ( $CDCl_3$ ):  $\delta$  1.44 (s, 18H,  $^tBu$ ), 2.17 (s, 6H, Me), 3.53 (s, 6H, OMe), 5.02 (s,  $^1H$ , CH,  $^2J(^{119}Sn-^1H) = 104$  Hz), 6.36 (2H,  $C_6H_2$ ), 6.96 (2H,  $C_6H_2$ ), 6.98–7.16 (complex pattern, 15H, SnPh, SPh).  $^{13}C$  NMR ( $CDCl_3$ ):  $\delta$  21.3 ( $CH_3$ ), 31.5 ( $C(CH_3)_3$ ), 40.9 (CH,  $^1J(^{119}Sn-^{13}C) = 430$  Hz), 35.1 ( $C(CH_3)_3$ ), 61.8 (OCH $_3$ ); phenyl carbons:  $\delta/J(^{119}Sn-^{13}C)$  155.3/45, 142.4/17, 142.0/526, 135.5/43, 135.3/15, 133.3/43, 132.9/16, 132.5/22, 130.4/38, 128.9/15, 128.2/62, 128.1, 126.2/19, 126.0/8 Hz.

**Synthesis of Cl $_3$ SnL (7).** Dry HCl gas was bubbled for 30 min through a solution of **1** (1.0 g, 1.4 mmol) in 100 mL of  $CHCl_3$  at 0 °C. The solution was then stirred at ambient temperature for 5 days, after which evaporation of the  $CHCl_3$  afforded a purple oil. The oil was dissolved in hexane (10 mL) and left to stand in a refrigerator overnight to yield 0.68 g (82%) of **7** as a white solid, mp 155–156 °C. Anal. Calcd for  $C_{25}H_{35}O_2SnCl_3$  (MW 592.63): C, 50.50; H, 6.27; Cl, 17.89. Found: C, 50.24; H, 6.08; Cl, 18.07.  $^1H$  NMR ( $CDCl_3$ ):  $\delta$  1.43 (s, 18H,  $^tBu$ ), 2.28 (s, 6H, Me), 3.62 (s, 6H, OMe), 4.82 (s,  $^1H$ ,

CH,  $^1J(^{119}\text{Sn}-^1\text{H}) = 127$  Hz), 6.75 (s, 2H, C<sub>6</sub>H<sub>2</sub>), 7.20 (s, 2H, C<sub>6</sub>H<sub>2</sub>).  $^{13}\text{C}$  NMR (CDCl<sub>3</sub>):  $\delta$  21.1 (CH<sub>3</sub>), 31.6 (C(CH<sub>3</sub>)<sub>3</sub>), 35.2 (C(CH<sub>3</sub>)<sub>3</sub>), 49.7 (CH,  $^1J(^{119}\text{Sn}-^{13}\text{C}) = 860$  Hz), 64.5 (OCH<sub>3</sub>), C<sub>6</sub>H<sub>2</sub> (not assigned), 129.1, 129.4, 131.1, 134.2, 142.7, 153.7.

**Synthesis of (2-MeO-3<sup>t</sup>Bu-5-Me-C<sub>6</sub>H<sub>2</sub>)<sub>2</sub>CHCH<sub>2</sub>Br, (LCH<sub>2</sub>)-Br (**8**).** To a chilled solution (-20 °C) of (2-MeO-3<sup>t</sup>Bu-5-MeC<sub>6</sub>H<sub>2</sub>)<sub>2</sub>CH<sub>2</sub> (10.82 g, 29.4 mmol) and 150 mL of dry THF, *n*-butyllithium (16.32 mL, 1.8 M) was added dropwise. The reaction mixture was maintained at -20 °C for 2 h and then cooled to -55 °C. Formaldehyde gas, generated by heating dry *para*-formaldehyde, was passed over the orange solution until it faded to pale yellow. The reaction mixture was stirred overnight at ambient temperature. Then the THF was distilled off. Ether (100 mL) was added, and the solution was hydrolyzed with 25 mL of 1.0 M HCl under ice cooling. The organic layer was separated and washed with 20 mL of 1.0 M HCl, 20 mL of H<sub>2</sub>O, and 20 mL of 10% K<sub>2</sub>CO<sub>3</sub>. The ether solution was then dried over anhydrous potassium carbonate. Evaporation of the ether gave a clear oil, which was dissolved in hexane/ether (50:50) and placed in a refrigerator overnight to afford 9.12 g (78%) of (2-MeO-3<sup>t</sup>Bu-5-Me-C<sub>6</sub>H<sub>2</sub>)<sub>2</sub>CHCH<sub>2</sub>OH as a colorless crystalline solid, mp 70–72 °C.  $^1\text{H}$  NMR (CDCl<sub>3</sub>):  $\delta$  1.39 (s, 18H, <sup>t</sup>Bu), 2.29 (s, 6H, Me), 3.78 (s, 6H, OMe), 4.02 ( $\delta$ , 2H, CH<sub>2</sub>), 5.02 (t, <sup>1</sup>H, CH), 6.98 (s, <sup>1</sup>H), 6.98 (s, 2H, C<sub>6</sub>H<sub>2</sub>), 7.02 (s, 2H, C<sub>6</sub>H<sub>2</sub>).

A solution of (2-MeO-3<sup>t</sup>Bu-5-Me-C<sub>6</sub>H<sub>2</sub>)<sub>2</sub>CHCH<sub>2</sub>OH (2.5 g, 6.72 mmol), PPh<sub>3</sub> (1.65 g, 6.72 mmol), and CBr<sub>4</sub> (2.08 g, 6.72 mmol) in toluene was prepared by adding each component in small portions. The solution was heated at reflux overnight and the resulting liquid was filtered. The toluene filtrate was evaporated in vacuo and replaced with 25 mL of hexane, then filtered once again. The resulting hexane filtrate was evaporated in vacuo to leave an orange oil, which was dissolved in methanol and placed in a refrigerator overnight to afford 2.38 g (83%) of **8** as a colorless crystalline solid, mp 94–96 °C. Anal. Calcd for C<sub>26</sub>H<sub>37</sub>O<sub>2</sub>Br (MW 461.52): C, 67.66; H, 8.08; Br, 17.31. Found: C, 67.82; H, 7.89; Br, 17.22.  $^1\text{H}$  NMR (CDCl<sub>3</sub>):  $\delta$  1.41 (s, 18H, <sup>t</sup>Bu), 2.25 (s, 6H, Me), 3.81 (s, 6H, OMe), 3.88 ( $\delta$ , 2H, CH<sub>2</sub>), 5.16 (t, <sup>1</sup>H, CH), 6.83 (s, 2H, C<sub>6</sub>H<sub>2</sub>), 7.09 (s, 2H, C<sub>6</sub>H<sub>2</sub>).  $^{13}\text{C}$  NMR (CDCl<sub>3</sub>):  $\delta$  21.4 (CH<sub>3</sub>), 35.6 (CH<sub>2</sub>), 31.3 (C(CH<sub>3</sub>)<sub>3</sub>), 35.1 (CH), 40.8 (C(CH<sub>3</sub>)<sub>3</sub>), 62.2 (OMe), C<sub>6</sub>H<sub>2</sub> (not assigned), 127.2, 127.4, 132.4, 134.5, 142.9, 156.4.

**Synthesis of Ph<sub>3</sub>Sn(CH<sub>2</sub>L) (**9**).** To a solution of Ph<sub>3</sub>SnNa in liquid ammonia at -78 °C, prepared from Ph<sub>3</sub>SnCl (3.34 g, 8.67 mmol) and sodium (0.398 g, 8.67 mmol), was added **8** (4.00 g, 8.67 mmol) dissolved in 40 mL of dry THF. After 30 min at -78 °C, the reaction mixture was left to stir overnight at ambient temperature. Then most of the THF was distilled off. Ether (60 mL) was added, and the solution was hydrolyzed with ice cooling. The organic layer was separated, and the aqueous layer was extracted three times with 15 mL of ether. The combined organic layers were dried over magnesium sulfate. The ether was evaporated, and the clear oil was dissolved in 50 mL of hexane, which upon cooling in a refrigerator afforded 4.92 g (78%) of **9** as a colorless crystalline solid, mp 135–137 °C. Anal. Calcd for C<sub>44</sub>H<sub>52</sub>O<sub>2</sub>Sn (MW 731.63): C, 72.24; H, 7.16. Found: C, 72.04; H, 7.19.  $^1\text{H}$  NMR (CDCl<sub>3</sub>):  $\delta$  1.34 (s, 18H, <sup>t</sup>Bu), 2.07 (s, 6H, Me), 3.49 (s, 6H, OMe), 2.27 ( $\delta$ , 2H, CH<sub>2</sub>),  $^2J(^{119}\text{Sn}-^1\text{H}) = 52$  Hz), 5.13 (t, <sup>1</sup>H, CH), 6.92 (s, 2H, C<sub>6</sub>H<sub>2</sub>), 6.95 (s, 2H, C<sub>6</sub>H<sub>2</sub>), 7.18–7.51 (complex pattern, 15H, SnPh).  $^{13}\text{C}$  NMR (CDCl<sub>3</sub>):  $\delta$  21.2 (CH<sub>3</sub>), 22.4 (CH<sub>2</sub>,  $^1J(^{119}\text{Sn}-^{13}\text{C}) = 377$  Hz), 31.4 (C(CH<sub>3</sub>)<sub>3</sub>), 34.8 (CH), 35.1 (C(CH<sub>3</sub>)<sub>3</sub>), 61.9 (OMe), C<sub>6</sub>H<sub>2</sub> (not assigned), 126.4, 128.5, 132.4, 137.5, 142.6, 155.4; SnPh<sub>3</sub> 140.1 (C<sub>j</sub>), 137.0 (C<sub>o</sub>), 128.5 (C<sub>m</sub>), 128.1 (C<sub>p</sub>).

**Synthesis of PhCl<sub>2</sub>Sn(CH<sub>2</sub>L) (**10**).** To a solution of **9** (0.7 g, 0.957 mmol) in 30 mL of acetone at 0 °C, HgCl<sub>2</sub> (0.520 g, 1.92 mmol) was added in portions. The solution was stirred at this temperature for 15 min and then stirred overnight at ambient temperature. The reaction mixture was evaporated in vacuo, and 20 mL of dichloromethane was added to the residue. The solution was placed in the freezer overnight, then

filtered. The clear dichloromethane filtrate was reduced to approximately 10 mL, and the solution was placed in the freezer overnight. The solution was again filtered, the dichloromethane filtrate was evaporated in vacuo, and the residue was recrystallized from hexane to afford 0.52 g (84%) of **10**, mp 125–127 °C. Anal. Calcd for C<sub>32</sub>H<sub>42</sub>O<sub>2</sub>SnCl<sub>2</sub> (MW 648.32): C, 59.29; H, 6.53; Cl, 10.94. Found: C, 59.03; H, 6.61; Cl, 10.40.  $^1\text{H}$  NMR (CDCl<sub>3</sub>):  $\delta$  1.31 (s, 18H, <sup>t</sup>Bu), 2.21 (s, 6H, Me), 3.68 (s, 6H, OMe), 2.27 ( $\delta$ , 2H, CH<sub>2</sub>),  $^2J(^{119}\text{Sn}-^1\text{H}) = 74$  Hz), 5.20 (t, <sup>1</sup>H, CH), 6.92 (s, 2H, C<sub>6</sub>H<sub>2</sub>), 6.95 (s, 2H, C<sub>6</sub>H<sub>2</sub>), 7.28–7.60 (complex pattern, 5H, SnPh).  $^{13}\text{C}$  NMR (CDCl<sub>3</sub>):  $\delta$  21.2 (CH<sub>3</sub>), 37.1 (CH<sub>2</sub>,  $^1J(^{119}\text{Sn}-^{13}\text{C}) = 542$  Hz), 31.5 (C(CH<sub>3</sub>)<sub>3</sub>), 34.2 (CH), 35.2 (C(CH<sub>3</sub>)<sub>3</sub>), 62.7 (OMe), C<sub>6</sub>H<sub>2</sub> (not assigned), 127.3, 127.9, 134.2, 138.0, 143.2, 154.8; SnPh 140.4 (C<sub>j</sub>), 133.4 (C<sub>o</sub>), 130.7 (C<sub>m</sub>), 128.9 (C<sub>p</sub>).

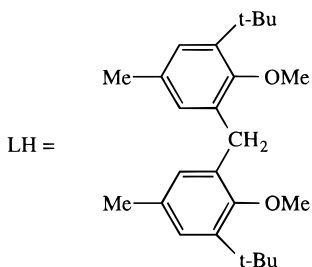
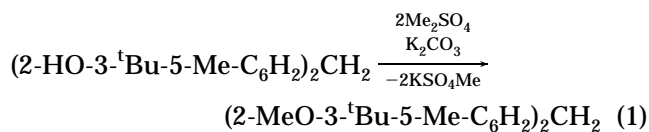
**Synthesis of PhBr<sub>2</sub>Sn(CH<sub>2</sub>L) (**11**).** To a solution of **9** (0.4 g, 0.547 mmol) in 15 mL of toluene at -78 °C, bromine (0.175 g, 1.09 mmol) in 10 mL of methanol was added. The solution was stirred at this temperature for 25 min and then stirred for a further 2 h at ambient temperature. The solution was evaporated in vacuo, and the residue was recrystallized from hexane to yield 0.31 g (77%) of **11** as a colorless solid, mp 133–135 °C. Anal. Calcd for C<sub>32</sub>H<sub>42</sub>O<sub>2</sub>SnBr<sub>2</sub> (MW 737.23): C, 52.14; H, 5.74; Br 21.68. Found: C, 51.62; H, 5.73; Br, 21.91.  $^1\text{H}$  NMR (CDCl<sub>3</sub>):  $\delta$  1.33 (s, 18H, <sup>t</sup>Bu), 2.14 (s, 6H, Me), 3.69 (s, 6H, OMe), 2.85 ( $\delta$ , 2H, CH<sub>2</sub>),  $^2J(^{119}\text{Sn}-^1\text{H}) = 65$  Hz), 5.24 (t, <sup>1</sup>H, CH), 6.89 (s, 2H, C<sub>6</sub>H<sub>2</sub>), 6.99 (s, 2H, C<sub>6</sub>H<sub>2</sub>), 7.13–7.50 (complex pattern, 5H, SnPh).  $^{13}\text{C}$  NMR (CDCl<sub>3</sub>):  $\delta$  21.2 (CH<sub>3</sub>), 38.4 (CH<sub>2</sub>,  $^1J(^{119}\text{Sn}-^{13}\text{C}) = 484$  Hz), 31.4 (C(CH<sub>3</sub>)<sub>3</sub>), 34.8 (CH), 35.2 (C(CH<sub>3</sub>)<sub>3</sub>), 62.5 (OMe), C<sub>6</sub>H<sub>2</sub> (not assigned), 127.3, 128.7, 134.1, 137.8, 143.2, 155.2; SnPh 139.7 (C<sub>j</sub>), 133.2 (C<sub>o</sub>), 130.6 (C<sub>m</sub>), 127.6 (C<sub>p</sub>).

**Synthesis of PhI<sub>2</sub>Sn(CH<sub>2</sub>L) (**12**).** To a solution of **9** (0.7 g, 0.957 mmol) in 25 mL of dichloromethane, iodine (0.493 g, 1.92 mmol) was added in portions over 15 min. After the reaction mixture was stirred overnight, the solution was evaporated in vacuo and the residue dissolved in hexane and placed in a refrigerator to precipitate 0.63 g (79%) of **12** as an orange oil. Anal. Calcd for C<sub>32</sub>H<sub>42</sub>O<sub>2</sub>SnI<sub>2</sub> (MW 831.22): C, 46.24; H, 5.09; I, 30.54. Found: C, 46.12; H, 5.18; I, 30.65.  $^1\text{H}$  NMR (CDCl<sub>3</sub>):  $\delta$  1.49 (s, 18H, <sup>t</sup>Bu), 2.20 (s, 6H, Me), 3.83 (s, 6H, OMe), 3.07 ( $\delta$ , 2H, CH<sub>2</sub>),  $^2J(^{119}\text{Sn}-^1\text{H}) = 54$  Hz), 5.34 (t, <sup>1</sup>H, CH), 6.99 (s, 2H, C<sub>6</sub>H<sub>2</sub>), 7.08 (s, 2H, C<sub>6</sub>H<sub>2</sub>), 7.21–7.64 (complex pattern, 5H, SnPh).  $^{13}\text{C}$  NMR (CDCl<sub>3</sub>):  $\delta$  21.3 (CH<sub>3</sub>), 38.1 (CH<sub>2</sub>,  $^1J(^{119}\text{Sn}-^{13}\text{C}) = 392$  Hz), 31.3 (C(CH<sub>3</sub>)<sub>3</sub>), 35.0 (CH), 35.7 (C(CH<sub>3</sub>)<sub>3</sub>), 62.3 (OMe), C<sub>6</sub>H<sub>2</sub> (not assigned), 128.3, 134.1, 137.3, 143.0, 155.4; SnPh (not assigned due to overlapping) 127.2, 130.1, 132.8.

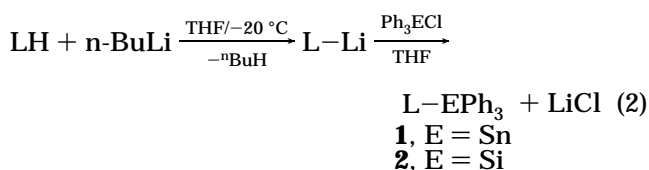
**Synthesis of Cl<sub>3</sub>Sn(CH<sub>2</sub>L) (**13**).** To a solution of **9** (1.0 g, 1.37 mmol) in 100 mL of chloroform at 0 °C was bubbled dry HCl gas for 30 min. The flask was removed from the cooling bath and a stopper fixed securely. The solution was then stirred at ambient temperature for 5 days, after which evaporation of the chloroform afforded a clear oil. The oil was dissolved in hexane and left to stand in a refrigerator overnight to yield 0.62 g (75%) of **13** as a colorless solid, mp 187–189 °C. Anal. Calcd for C<sub>26</sub>H<sub>37</sub>O<sub>2</sub>SnCl<sub>3</sub> (MW 606.66): C, 51.48; H, 6.15; Cl, 17.53. Found: C, 51.14; H, 5.87; Cl, 17.52.  $^1\text{H}$  NMR (CDCl<sub>3</sub>):  $\delta$  1.43 (s, 18H, <sup>t</sup>Bu), 2.29 (s, 6H, Me), 3.77 (s, 6H, OMe), 2.82 ( $\delta$ , 2H, CH<sub>2</sub>),  $^2J(^{119}\text{Sn}-^1\text{H}) = 85$  Hz), 5.16 (t, <sup>1</sup>H, CH), 6.88 (s, 2H, C<sub>6</sub>H<sub>2</sub>), 7.15 (s, 2H, C<sub>6</sub>H<sub>2</sub>).  $^{13}\text{C}$  NMR (CDCl<sub>3</sub>):  $\delta$  21.4 (CH<sub>3</sub>), 41.9 (CH<sub>2</sub>,  $^1J(^{119}\text{Sn}-^{13}\text{C}) = 750$  Hz), 31.7 (C(CH<sub>3</sub>)<sub>3</sub>), 34.6 (CH), 35.6 (C(CH<sub>3</sub>)<sub>3</sub>), 63.6 (OMe), C<sub>6</sub>H<sub>2</sub> (not assigned), 127.6, 129.0, 134.1, 136.2, 143.3, 155.0.

## Results and Discussion

**Syntheses.** Methylation of bis(2-hydroxy-3-*tert*-butyl-5-methylphenyl)methane, using Me<sub>2</sub>SO<sub>4</sub>/K<sub>2</sub>CO<sub>3</sub> in acetone solution affords bis(2-methoxy-3-*tert*-butyl-5-methylphenyl)methane (LH) in good yield (eq 1).

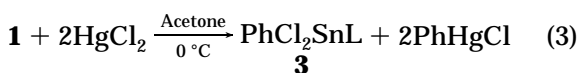


Compounds **1** and **2** were prepared as white crystalline solids in good yield from reaction of LH with <sup>n</sup>BuLi followed by addition of Ph<sub>3</sub>SnCl and Ph<sub>3</sub>SiCl, respectively, eq 2. Deuterium labeling experiments indicated

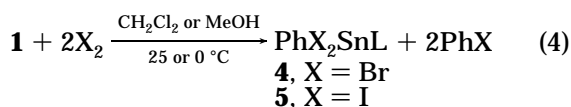


that metalation of LH is best performed in THF at -20 °C (no attack of the solvent was observed at this temperature, but at 0 °C rapid decomposition was observed). Attempts to metalate diphenylmethane under the same reaction conditions were not successful and indicate that the methoxy groups in LH stabilize the lithiated species, LiL.

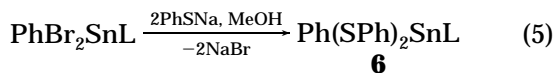
Reaction of **1** with 2 equiv of HgCl<sub>2</sub> cleaves two phenyl groups to give **3** in high yield (eq 3). Compounds **4** and



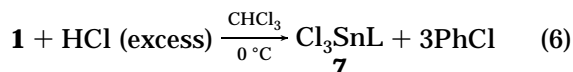
**5** were prepared in excellent yields by reaction of **1** with 2 equiv of Br<sub>2</sub> and I<sub>2</sub>, respectively (eq 4). The thiophe-



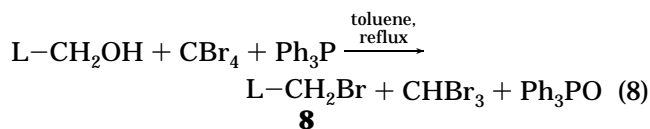
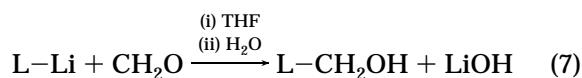
nolate **6** was prepared by reaction of **4** with 2 equiv of sodium thiolate (eq 5).



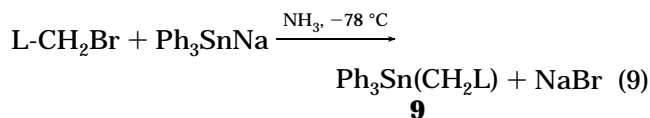
Attempts to cleave the remaining phenyl group from compounds **3**–**5** using an additional equivalent of the respective reagents were not successful. However, cleavage of all three phenyl groups was achieved by stirring **1** in a saturated solution of CHCl<sub>3</sub>/HCl for 5 days, producing **7** as a white solid (eq 6).



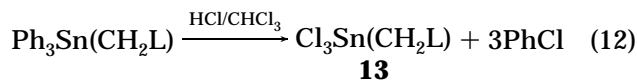
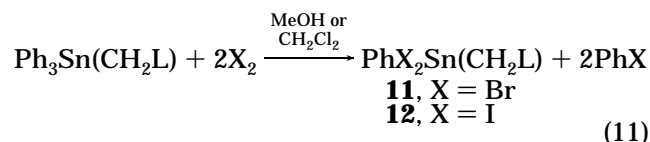
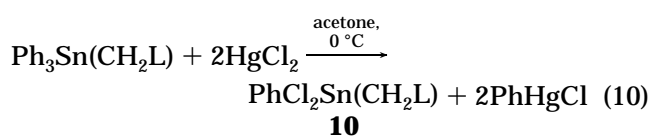
In order to synthesize a ligand which potentially would give rise to a six-membered chelate L-Li was reacted with formaldehyde followed by bromination to give **8** (eqs 7 and 8). The formation of LCH<sub>2</sub>SnPh<sub>3</sub> (**9**)



was achieved by reaction of **8** with sodium triphenylstannide, Ph<sub>3</sub>SnNa, in liquid ammonia (eq 9). Func-



tionalization at tin was achieved in good yield by reaction of **9** with HgCl<sub>2</sub> or either Br<sub>2</sub> or I<sub>2</sub> (eqs 10 and 11), whereas treatment of **9** with excess HCl afforded compound **13** (eq 12).



Compounds **1**–**11** and **13** are colorless solids, whereas **12** is an oil. All compounds show good solubility in common organic solvents, such as CH<sub>2</sub>Cl<sub>2</sub>, THF, and toluene.

**Molecular Structures of 1–6.** The molecular structures of **1**, **2**, **3**, and **6** are shown in Figures 1–4, respectively, and selected interatomic parameters of all structures are collected in Table 2; a common numbering scheme was employed for compounds **3**–**5**. The structures are molecular with no significant intermolecular contacts in their respective crystal lattices. The structures fall neatly into two categories with the first featuring four-coordinate tin (or silicon) atom geometries. The tin (silicon) atom in **1** (**2**) is coordinated by three phenyl substituents and the tertiary carbon atom of L with the Sn–C(1) (Si–C(1)) bond being significantly longer at 2.182(6) Å (1.925(4) Å) than the Sn–C(Ph) (Si–C(Ph)) bonds which lie in the range 2.102(7)–2.122(7) Å (1.871(4)–1.884(4) Å). The angles subtended at the tin (silicon) atom lie in the relatively narrow range of 107.0(2)–112.9(2)° (107.3(2)–113.3(2)°), indicating that any deviation from the ideal tetrahedral geometry is small. The coordination environment about the tin (silicon) atom is consistent with the absence of a significant intramolecular interaction between the methoxy oxygen atoms and the central atom. Thus, in **1** the Sn···O(1) and Sn···O(2) separations are 3.023(4) and 4.406(5) Å, respectively, and the analogous separations in **2** are 4.442(3) and 3.857(3) Å, respectively. The Sn···O(1) separation is shorter than the sum of the van der Waals radii for these atoms of 3.5 Å, and further

**Table 2. Selected Interatomic Bond Distances (Å) and Angles (deg) for 1–6**

	<b>1</b>	<b>2<sup>a</sup></b>	<b>3</b>	<b>4</b>	<b>5</b>	<b>6<sup>b</sup></b>
	X = C(31) Y = C(51)	X = C(31) Y = C(51)	X = Cl(1) Y = Cl(2)	X = Br(1) Y = Br(2)	X = I(1) Y = I(2)	X = S(1) Y = S(2)
Sn–X	2.122(7)	1.873(4)	2.321(2)	2.494(2)	2.702(1)	2.417(2)
Sn–Y	2.102(7)	1.884(4)	2.355(2)	2.526(2)	2.736(1)	2.419(2)
Sn–C(1)	2.182(6)	1.925(4)	2.164(5)	2.21(1)	2.23(1)	2.187(5)
Sn–C(41)	2.118(7)	1.871(4)	2.108(6)	2.15(1)	2.15(1)	2.135(6)
Sn–O(1)			2.559(4)	2.630(7)	2.684(7)	2.989(4)
O(1)–C(12)	1.378(7)	1.396(4)	1.391(6)	1.41(1)	1.41(1)	1.395(7)
O(2)–C(22)	1.382(7)	1.394(4)	1.392(6)	1.40(1)	1.39(1)	1.396(6)
X–Sn–Y	108.8(3)	107.3(2)	102.39(8)	104.13(6)	107.30(4)	109.22(7)
X–Sn–C(1)	107.0(2)	109.5(2)	105.1(2)	105.5(3)	107.3(3)	113.4(2)
X–Sn–C(41)	107.1(3)	108.7(2)	104.4(2)	105.2(3)	105.0(3)	101.6(2)
X–Sn–O(1)			87.5(1)	86.7(2)	88.4(1)	83.80(9)
Y–Sn–C(1)	111.6(2)	108.5(2)	101.7(2)	101.2(3)	100.6(3)	103.5(1)
Y–Sn–C(41)	109.2(3)	109.3(2)	99.9(2)	101.1(4)	100.8(3)	108.7(2)
Y–Sn–O(1)			168.35(9)	167.3(2)	162.9(1)	164.56(8)
C(1)–Sn–C(41)	112.9(2)	113.3(2)	138.4(2)	135.8(4)	133.5(4)	120.2(2)
C(1)–Sn–O(1)			69.3(2)	69.1(3)	67.4(3)	62.7(2)
C(41)–Sn–O(1)			83.3(2)	81.9(4)	81.0(4)	75.5(2)
Sn–C(1)–C(11)	110.9(4)	114.0(2)	108.0(3)	107.7(7)	108.4(6)	111.5(3)
Sn–C(1)–C(21)	109.5(4)	111.7(2)	110.1(3)	107.8(7)	107.7(7)	111.6(4)
C(11)–C(1)–C(21)	116.6(5)	112.7(3)	115.9(5)	119(1)	116.6(9)	114.9(4)
C(12)–O(1)–C(12')	115.3(5)	114.4(3)	113.5(5)	113.2(9)	112.2(8)	115.0(5)
C(22)–O(2)–C(22')	115.3(6)	115.4(3)	113.8(4)	113.3(8)	114.8(8)	114.5(5)
C(1)/C(11)/C(12)/O(1)	4.4(9)	5.4(5)	–4.2(6)	–4(2)	3(1)	5.0(8)
C(1)/C(21)/C(22)/O(2)	–2.0(9)	8.7(5)	6.8(7)	3(2)	7(1)	–0.8(8)
C(12)/C(11)/C(1)/C(21)	179.6(6)	100.5(4)	–161.9(4)	–160(1)	–165.0(9)	178.0(5)
C(11)/C(1)/C(21)/C(22)	117.3(7)	–140.0(3)	–126.1(5)	–126(1)	–129(1)	106.2(6)

<sup>a</sup> For Sn read Si. <sup>b</sup> For C(41) read C(51).

evidence for a weak interaction is found in the magnitude of the C(11)–C(12)–O(1) angle of 116.0(6)° (concomitantly, the C(13)–C(12)–O(1) angle is 119.8(6)°), which is approximately 2° smaller than the C–C–O(2) angles and the comparable angles in **2**, and indicates that the O(1) atom is being pulled toward the tin atom. Such weak Sn···O interactions have been described in related studies on intramolecular Sn···O in tetraorganotin.<sup>8a</sup> In contrast to the structure of **1** (and of **2**), generally significant intramolecular interactions are found in the remaining structures where two of the tin-bound phenyl groups have been substituted for X = Cl (**3**), Br (**4**), I (**5**), and SPh (**6**).

In each of the structures of **3–6** the tin atom is coordinated by a phenyl substituent, two donor atoms X, the C(1) atom, as well as the O(1) atom derived from L. In each case, the Sn···O(1) contact is longer than a normal covalent Sn–O bond; however, the resulting tin atom geometry, i.e., distorted trigonal bipyramidal, clearly indicates the presence of a significant Sn···O(1) interaction. The O(1) and X(2) atoms define the axial angle in this description, and the tin atom lies 0.4186(4), 0.4638(8), 0.4938(8), and 0.5279 (4) Å out of the trigonal plane in the direction of the X(2) atom, respectively, for **3–6**. The distortion from the ideal trigonal bipyramidal geometry correlates with the magnitude of the Sn···O(1) interaction, i.e., the weaker the interaction the greater the distortion toward a tetrahedral geometry about the tin atom. Thus, the length of the Sn···O(1) distance increases from 2.559(4) Å for **3**, 2.630(7) Å for **4**, 2.684(7) Å for **5** to a maximum of 2.989(4) Å for **6** and suggests an order for the Lewis acidity for the tin-containing entities, i.e., PhSnCl<sub>2</sub> > PhSnBr<sub>2</sub> > PhSnI<sub>2</sub> > PhSn(SPh)<sub>2</sub>. By contrast to the Sn···O(1) contacts, the Sn···O(2) interactions are not significant at 4.344(4), 4.347(7), 4.365(7), and 4.621(4) Å for **3–6**, respectively. As a consequence of the diminished strength of the Sn···O(1) interaction in **3–6**, there are other systematic

**Table 3. <sup>119</sup>Sn NMR Data for Compounds 1 and 3–6**

compd	T, °C	δ( <sup>119</sup> Sn), ppm	solvent
<b>1</b>	25	–114.6	CH <sub>2</sub> Cl <sub>2</sub>
	–80	–114.0	CH <sub>2</sub> Cl <sub>2</sub>
<b>3</b>	+100	–83.4	toluene
	+25	no signal	CH <sub>2</sub> Cl <sub>2</sub>
	–25	–69.5, –122.0	CH <sub>2</sub> Cl <sub>2</sub>
	–55	–71.0, –125.1	CH <sub>2</sub> Cl <sub>2</sub>
	–80	–132.4	CH <sub>2</sub> Cl <sub>2</sub>
<b>4</b>	+100	–82.7	toluene
	+25	no signal	CH <sub>2</sub> Cl <sub>2</sub>
	–25	–60.2, –148.2	CH <sub>2</sub> Cl <sub>2</sub>
	–55	–59.8, –148.7	CH <sub>2</sub> Cl <sub>2</sub>
	–100	–63.8, –150.7	CH <sub>2</sub> Cl <sub>2</sub>
<b>5</b>	+100	–153.9	toluene
	+75	–146.0	toluene
	+25	–129.3	toluene
	–90	–91.3	toluene
<b>6</b>	+25	12.0	CH <sub>2</sub> Cl <sub>2</sub>
	–55	17.5	CH <sub>2</sub> Cl <sub>2</sub>

changes in the tin atom geometry, i.e., there is a general increase in the X–Sn–Y and X–Sn–C(1) angles and a general decrease in the C(1)–Sn–C(41), C(1)–Sn–O(1), and C(41)–Sn–O(1) angles (see Table 2).

**NMR Studies.** The <sup>119</sup>Sn NMR (CH<sub>2</sub>Cl<sub>2</sub>) data for **1** indicate the tin atom is four-coordinate at room temperature as well as at –80 °C (Table 3). The <sup>1</sup>J(<sup>119</sup>Sn–<sup>13</sup>CH) and <sup>1</sup>J(<sup>119</sup>Sn–<sup>13</sup>C<sub>i</sub>), couplings of 380 and 481 Hz, respectively, also indicate four-coordinate tin. A comparable four coordinate species, Ph<sub>3</sub>SnCH<sub>3</sub>, has a δ(<sup>119</sup>Sn) of –98.0 ppm,<sup>14</sup> and <sup>1</sup>J(<sup>119</sup>Sn–<sup>13</sup>C) and <sup>1</sup>J(<sup>119</sup>Sn–<sup>13</sup>C<sub>i</sub>) couplings of 374 and 511 Hz, respectively.<sup>15</sup> The isotropic <sup>119</sup>Sn chemical shift of **1** in the solid state, δ<sub>iso</sub> –101 ppm, indicates there is little difference between the solution and solid state structures.

(14) Wrackmeyer, B. *Ann. Rep. NMR Spectrosc.* **1985**, *16*, 73.

(15) Mitchell, T. N.; Walter, G. J. *Organomet. Chem.* **1976**, *121*, 177.

At room temperature, the  $^1\text{H}$  and  $^{13}\text{C}$  NMR spectra of **1** show one resonance for the respective homologous substituents on both ligand phenyl rings. On cooling to  $-110\text{ }^\circ\text{C}$ , the  $^{13}\text{C}$  NMR resonances become very broad. The  $^1\text{H}$  NMR spectrum does show splitting at  $-110\text{ }^\circ\text{C}$ , indicating two types of methoxy groups (3.45, 3.55 ppm), methyl groups (1.56, 2.15 ppm), and  $t\text{Bu}$  groups (0.92, 1.32 ppm). Only one methine proton is present (4.89 ppm,  $^2J(^{119}\text{Sn}-^1\text{H}) = 101\text{ Hz}$ ), and a complex pattern is observed in the aromatic region. These data are consistent with rapid rotation of the ligand  $[\text{Me}^t\text{BuOMeC}_6\text{H}_2]$  groups about their central methine carbon at room temperature. Lowering the temperature slows this rotation, and at  $-110\text{ }^\circ\text{C}$ , the two ligand  $[\text{Me}^t\text{BuOMeC}_6\text{H}_2]$  groups in compound **1** become nonequivalent, presumably adopting an orthogonal relationship as was observed in the solid state structure. This was confirmed by the solid state  $^{13}\text{C}$  NMR of **1** which showed two distinct signals for each of the substituents on the aromatic ligand rings.

Interestingly, the  $^1\text{H}$  and  $^{13}\text{C}$  NMR spectra of LH and of the silicon compound, **2**, indicate free rotation of the  $[\text{Me}^t\text{BuOMeC}_6\text{H}_2]$  down to  $-110\text{ }^\circ\text{C}$ . This indicates that the restricted rotation observed for **1** is a consequence of the residual Lewis acidity at tin rather than of steric hindrance.

The  $^{119}\text{Sn}$  NMR spectrum of  $\text{PhBr}_2\text{SnL}$ , **4** (Table 3), in toluene at  $100\text{ }^\circ\text{C}$  shows one resonance ( $-82.7\text{ ppm}$ ), which on cooling begins to broaden at  $50\text{ }^\circ\text{C}$ . No  $^{119}\text{Sn}$  NMR resonance is observed at  $25\text{ }^\circ\text{C}$ , but at  $-25\text{ }^\circ\text{C}$  two broad signals appear at  $-60.2$  and  $-148.2\text{ ppm}$ . At  $-55\text{ }^\circ\text{C}$  these signals both sharpen ( $-59.8$  and  $-148.7\text{ ppm}$ ), and at  $-100\text{ }^\circ\text{C}$  the higher frequency signal becomes very broad while the lower frequency signal remains sharp. The relative intensities of the two  $^{119}\text{Sn}$  NMR resonances vary with temperature. A ratio of 2:1 in favor of the higher frequency peak is observed at  $-25\text{ }^\circ\text{C}$ . This becomes a 1:1 ratio at  $-100\text{ }^\circ\text{C}$ .

At  $25\text{ }^\circ\text{C}$ , the  $^1\text{H}$  and  $^{13}\text{C}$  NMR spectra of compound **4** show one resonance for each of the substituents of the aromatic ligand rings. At  $-110\text{ }^\circ\text{C}$ , the  $^1\text{H}$  NMR spectrum shows two types of methine protons at 4.47 and 5.07 ppm, having  $^2J(^{119}\text{Sn}-^1\text{H})$  couplings of 120 and 93 Hz, respectively. Additionally, four types of methoxy protons, four types of methyl protons, and three types of *tert*-butyl protons are observed. All signals are of approximately equal intensity.

The  $^{13}\text{C}$  NMR spectrum of **4** at  $-80\text{ }^\circ\text{C}$  shows two types of methine carbons (42.33 and 44.31 ppm, having  $^1J(^{119}\text{Sn}-^{13}\text{C})$  couplings of 561 and 652 Hz, respectively). Three types of methoxy carbons, two types of methyl carbons, two types of *tert*-butyl carbons ( $\text{C}(\text{CH}_3)_3$ ), and three types of quaternary carbons are observed. The aromatic region of the spectrum shows a complex set of signals.

The  $^{119}\text{Sn}$ ,  $^{13}\text{C}$ , and  $^1\text{H}$  NMR data indicate **4** exhibits two coordination states simultaneously in solution at low temperature, while at high temperature, an average of these coordination states is observed. Previous examples of two coordination states in organotin chemistry being observed simultaneously have been reported, however, such examples result from the coordination of an additional intermolecular donor molecule. For example, addition of a 0.5 mol equiv of pyridine to (2-[(dimethylamino)methyl]phenyl)phenyltin dichloride

results in simultaneous observation of five- and six-coordination states at low temperature.<sup>16</sup> Examples of temperature dependant coordination equilibria involving intramolecular coordination have also been reported, but these all exhibit rapid exchange between two coordination states at a given temperature. Such equilibria give rise to a single  $^{119}\text{Sn}$  NMR resonance which is an average of the population of the individual coordination states.<sup>16</sup> Unlike any previous examples, compound **4** exhibits a unique temperature-dependant equilibrium between two tin coordination states. At low temperature, the exchange appears slow on the NMR time scale and both coordination species are observed simultaneously. The  $^{119}\text{Sn}$  NMR chemical shift values of  $-59.8$  and  $-148.7\text{ ppm}$  ( $-55\text{ }^\circ\text{C}$ ) for **4** are assigned to four- and five-coordinate tin atoms, respectively, while that of  $-82.7\text{ ppm}$  ( $100\text{ }^\circ\text{C}$ ) is assigned to an average of both coordination states. Unfortunately, a solid state  $^{119}\text{Sn}$  NMR spectrum could not resolve these two species due to the very broad resonances ( $W_{1/2}$  approx 5 kHz, 45 ppm), although one isotropic peak appeared to be at  $\delta_{\text{iso}} -40\text{ ppm}$ .

The  $^1\text{H}-^{119}\text{Sn}$  2-D NMR spectrum shows that the lower frequency tin resonance at  $-148.7\text{ ppm}$  correlates to the methine proton resonance at 4.47 (correlation X) and the higher frequency tin resonance at  $-59.8\text{ ppm}$  to the methine proton resonance at 5.07 ppm (correlation Y). The  $^1\text{H}-^{13}\text{C}$  2-D NMR spectrum shows that the higher frequency methine carbon correlates to the lower frequency methine proton (correlation X) and the lower frequency methine carbon to the higher frequency methine proton (correlation Y). It is concluded that X and Y correlations represent resonances from the five- and four-coordinate tin species, respectively, in compound **4**.

The  $^{119}\text{Sn}$  NMR spectrum of the analogous dichloro compound,  $\text{PhCl}_2\text{SnL}$ , **3**, at  $-80\text{ }^\circ\text{C}$  shows only one resonance at  $-132.4\text{ ppm}$ . At  $-55\text{ }^\circ\text{C}$ , two resonances are observed at  $-71.0$  and  $-125.1\text{ ppm}$ , the former resonance being broad and of low intensity. The relative intensities of the two  $^{119}\text{Sn}$  NMR signals observed at  $-55\text{ }^\circ\text{C}$  is approximately 1:8 in favor of the lower frequency signal, this reduces to 1:5 at  $-25\text{ }^\circ\text{C}$ . No  $^{119}\text{Sn}$  NMR resonance is seen at  $25\text{ }^\circ\text{C}$ , but increasing the temperature to  $100\text{ }^\circ\text{C}$  gives a single sharp resonance at  $-83.4\text{ ppm}$ .

We conclude that compound **3** exhibits similar coordination properties to that observed for **4**; however, the equilibrium involving **3** favors the five-coordinate tin species. The  $^{119}\text{Sn}$  NMR resonance at  $-132.4\text{ ppm}$  ( $-80\text{ }^\circ\text{C}$ ) is assigned to the five-coordinate species. At  $-55\text{ }^\circ\text{C}$ , both four- and five-coordinate tin species are observed, with the major resonance at  $-125.1\text{ ppm}$  assigned to the five-coordinate tin species and that of the minor signal at  $-71.0\text{ ppm}$  to the four-coordinate tin species. The increased population of the five-coordinate species for **3** compared to **4** results from an increase in the Lewis acidity at the tin atom brought about by the more electronegative chlorine substituents. The solid state isotropic  $^{119}\text{Sn}$  NMR chemical shift of  $\delta_{\text{iso}} -132\text{ ppm}$  fits well with the pentacoordinate structure observed in the solid state for **3** and supports the interpretation of the low-temperature solution NMR data.

(16) Van Koten, G.; Jastrzebski, J. T. B. H.; Grove, D. M.; Boersma, J.; Ernsting, J. M. *Magn. Reson. Chem.* **1991**, *29*, 525.



Room-temperature  $^1\text{H}$  and  $^{13}\text{C}$  NMR spectra of **3** show equivalence of the respective ligand phenyl [ $\text{Me}^t\text{BuO-MeC}_6\text{H}_2$ ] groups about their central methine carbon at room temperature. At low temperature, both the  $^1\text{H}$  and  $^{13}\text{C}$  NMR spectra show the presence of both four- and five-coordinate tin species, with the intensities of the signals from the four-coordinate species being low.

In order to confirm the interpretation of the NMR results above and to exclude the existence of an ionic equilibrium,<sup>17</sup> such as  $\text{PhCl}_2\text{SnL} \rightleftharpoons [\text{PhClSn}]^+ \text{Cl}^-$  an equivalent molar ratio of **3** and **4** were dissolved in  $\text{CH}_2\text{Cl}_2$  and the  $^{119}\text{Sn}$  NMR spectrum of the resulting solution recorded at  $-55^\circ\text{C}$ . The  $^{119}\text{Sn}$  NMR spectrum contains seven signals ( $-64.1$ ,  $-74.5$ ,  $-85.3$ ,  $-129.8$ ,  $-130.6$ ,  $-146.9$ , and  $-148.1$  ppm). This indicates that ionic species are not present, since these could result in only five species in the mixture, i.e.,  $\text{PhCl}_2\text{SnL}$ ,  $\text{PhBr}_2\text{SnL}$ ,  $\text{PhClBrSnL}$ ,  $[\text{LSnPhCl}]^+\text{X}^-$ , and  $[\text{LSnPhBr}]^+\text{X}^-$  (where  $\text{X} = \text{Cl}$  or  $\text{Br}$ ). The  $^{119}\text{Sn}$  NMR experiment confirmed the presence of both four- and five-coordinate tin species with the above signals assigned as follows:  $\text{PhBr}_2\text{SnL}$ ,  $\text{PhBrClSnL}$ ,  $\text{PhCl}_2\text{SnL}$  (four-coordinate),  $\text{PhClBrSnL}$  (Br axial),  $\text{PhCl}_2\text{SnL}$ ,  $\text{PhBrClSnL}$  (Cl axial),  $\text{PhBr}_2\text{SnL}$  (five-coordinate), respectively. The  $^{119}\text{Sn}$  NMR chemical shift assignments of the five-coordinate species  $\text{LSnPhClBr}$  (Br axial) and  $\text{SnPhBrCl}$  (Cl axial) were made on the basis that the isomer with the strongest electron-donating group in the equatorial plane, i.e.,  $\text{PhBrClSnL}$  (Cl axial), would give rise to the tin resonance at lower frequency.<sup>18</sup>

The  $^{119}\text{Sn}$  NMR spectrum of  $\text{PhI}_2\text{SnL}$ , **5** (Table 3), at  $100^\circ\text{C}$  consists of a single sharp resonance at  $-153.9$  ppm. Lowering the temperature causes the signal to shift progressively toward higher frequency ( $-146.0$  ppm at  $75^\circ\text{C}$ ,  $-129.3$  ppm at  $25^\circ\text{C}$ ,  $-91.3$  ppm at  $-95^\circ\text{C}$ ). The resonance begins to broaden below  $-95^\circ\text{C}$ . Both  $^1\text{H}$  and  $^{13}\text{C}$  NMR spectra of **5** at  $25^\circ\text{C}$  show equivalence of the respective homologous substituents on the ligand phenyl groups. The resonances in the low-temperature  $^{13}\text{C}$  NMR spectrum are slightly broad. However, the low-temperature  $^1\text{H}$  NMR spectrum shows splitting of the resonances associated with the homologous ligand phenyl group substituents. As with compound **4**, the solid state  $^{119}\text{Sn}$  NMR spectrum of **5** showed very broad lines ( $W_{1/2} \approx 9$  kHz, 80 ppm), with one major species evident at  $\delta_{\text{iso}} -72$  ppm and both at room temperature and at 330 K.

A  $^{119}\text{Sn}$  shift which moves to lower frequency with an increase in temperature is unusual and requires comment. It is likely that **5** adopts a five-coordinate geometry at low temperature, similar to that observed in the solid state i.e., an essentially trigonal bipyramidal geometry in which one iodine atom occupies an axial position and the other iodine atom occupies an equatorial position. It has been suggested earlier that penta-coordinate tin(IV) complexes involve a secondary hybridization such that the s-character electron density is concentrated in the equatorial orbitals of the trigonal bipyramid.<sup>18–22</sup> Consequently, the nature of the donor

set in the equatorial plane, in this case  $\text{C}_2\text{I}$ , largely determines the  $^{119}\text{Sn}$  chemical shift of five-coordinate tin complexes.

Of the current series of **3–5**, the tin atom in **5** has the lowest Lewis acidity and is least likely to extend its coordination number through intramolecular coordination. This tendency is reflected in the X-ray crystal structures where **5** exhibits the weakest intramolecular Sn–O interaction (Table 2). Increasing the temperature promotes a rapid exchange of the methoxy donors at the tin atom, resulting in an essentially tetrahedral four-coordinate geometry in which there is a  $\text{C}_2\text{I}_2$  donor set about the tin. Iodine is highly polarizable and produces a very large shielding effect at tin.<sup>14</sup> Usually a decrease in coordination number is accompanied by  $^{119}\text{Sn}$  shifts to higher frequency. However, in this particular case, the change to lower coordination number which occurs with increasing temperature results in greater influence from the highly polarizable iodine atoms. The net result of these circumstances is a  $^{119}\text{Sn}$  NMR signal which shifts to lower frequency with a decrease in coordination number at tin.

**Reaction of Compounds 3–5 with Tributylphosphine Oxide.** In order to further examine the nature of the coordination equilibrium involved in solution for compounds **3–5**, their reaction with the strong Lewis base tributylphosphine oxide ( $\text{Bu}_3\text{PO}$ ) was studied. The  $^{119}\text{Sn}$  NMR spectrum ( $-80^\circ\text{C}$ ,  $\text{CH}_2\text{Cl}_2$ ) of a 1:1 mixture of  $\text{Bu}_3\text{PO}$  and **3** shows a doublet at  $-290.3$  ppm ( $^2J(^{119}\text{Sn}-^{31}\text{P}) = 205$  Hz). The spectrum remains the same when the ratio of  $\text{Bu}_3\text{PO}$  is increased to 4:1. No  $^{119}\text{Sn}$  NMR signals were observed at higher temperatures. These NMR data imply that **3** forms a 1:1 adduct with  $\text{Bu}_3\text{PO}$  ( $\text{PhCl}_2\text{SnL}\cdot\text{Bu}_3\text{PO}$ ) in situ at low temperature. The adduct is five-coordinate through intermolecular coordination of the phosphorus oxygen. Its  $^{119}\text{Sn}$  NMR chemical shift is consistent with other similar pentacoordinated species,<sup>18,23,24</sup> e.g.,  $\text{Ph}_2\text{SnCl}_2\cdot\text{Bu}_3\text{PO}$   $-276$  ppm,  $^2J(^{119}\text{Sn}-^{31}\text{P}) = 156$  Hz.<sup>18</sup> This result indicates that the intramolecular coordination of the methoxy group from the ligand has been replaced by a stronger intermolecular coordination from  $\text{Bu}_3\text{PO}$ . Higher adducts are not observed, even when the amount of  $\text{Bu}_3\text{PO}$  is increased to 4:1, implying that the maximum coordination number possible for this system is five. These data support the contention that the equilibria observed for **3** and **4** are indeed between four- and five- and not five- and six-coordinate tin species.

The  $^{119}\text{Sn}$  NMR spectrum ( $-80^\circ\text{C}$ ,  $\text{CH}_2\text{Cl}_2$ ) of a 1:1 mixture of  $\text{Bu}_3\text{PO}$  and **4** shows a doublet at  $-275.7$  ppm ( $^2J(^{119}\text{Sn}-^{31}\text{P}) = 196$  Hz). Increasing the ratio of  $\text{Bu}_3\text{PO}$  to 2:1 leaves the  $^{119}\text{Sn}$  NMR spectrum almost unchanged, with a low-intensity triplet (1:7) also being observed at  $-343.7$  ppm ( $^2J(^{119}\text{Sn}-^{31}\text{P}) = 233$  Hz). The spectrum is unaffected by increasing the amount of  $\text{Bu}_3\text{PO}$  to 4:1. No  $^{119}\text{Sn}$  NMR signals are observed at higher temperatures. Compound **4** also forms a 1:1 adduct with  $\text{Bu}_3\text{PO}$  ( $\text{PhBr}_2\text{SnL}\cdot\text{Bu}_3\text{PO}$ ) at low temperature, having a similar  $^{119}\text{Sn}$  NMR chemical shift to the

(17) Van Koten, G.; Jastrzebski, J. T. B. H.; Noltes, J. G.; Spek, A. L.; Schoone, J. C. *J. Organomet. Chem.* **1978**, *148*, 233.

(18) Colton, R.; Dakternieks, D. *Inorg. Chim. Acta.* **1985**, *102*, L17.

(19) Petrosyan, V. S.; Permin, A. B.; Reutov, O. A.; Roberts, J. D. *J. Magn. Reson.* **1980**, *40*, 511.

(20) Nadvornik, M.; Holecck, J.; Handliff, K.; Lycka, A. *J. Organomet. Chem.* **1984**, *275*, 43.

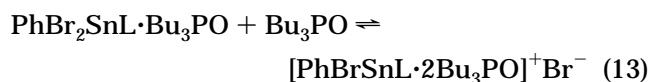
(21) Bent, H. A. *Chem. Rev.* **1961**, *61*, 275.

(22) Van Der Berghe, E. V.; Verdonck, L.; Van Der Kelen, G. P. *J. Organomet. Chem.* **1969**, *16*, 497.

(23) Smith, P. J.; Tupciauskas, A. P. *Ann. Rep. NMR Spectrosc.* **1978**, *8*, 291.

(24) *NMR and the Periodic Table*; Harris, R. K., Mann, B. E., Eds.; Academic Press: London, 1978; Chapter 10.

five-coordinate species  $\text{Ph}_2\text{SnBr}_2 \cdot \text{Bu}_3\text{PO}$  ( $-319$  ppm,  $^2J(^{119}\text{Sn}-^{31}\text{P}) = 166$  Hz).<sup>25</sup> The low-intensity triplet observed when the ratio of  $\text{Bu}_3\text{PO}$  is increased to 2:1 implies formation of an adduct containing two  $\text{Bu}_3\text{PO}$  groups. The  $^{119}\text{Sn}$  NMR chemical shift of this adduct is to higher frequency compared with the similar six-coordinate 1:2 adduct,  $\text{Ph}_2\text{SnBr}_2 \cdot 2\text{Bu}_3\text{PO}$  ( $-479$  ppm).<sup>25</sup> Additionally,  $\text{Ph}_2\text{SnBr}_2 \cdot 2\text{Bu}_3\text{PO}$  is known to undergo halide displacement upon coordination of a third  $\text{Bu}_3\text{PO}$  donor, i.e.,  $[\text{Ph}_2\text{SnBr} \cdot 3\text{Bu}_3\text{PO}]^+\text{Br}^-$ .<sup>25</sup> Thus, it is proposed that when the ratio of  $\text{Bu}_3\text{PO}$  is increased to 2:1, an equilibrium is established between the 1:1 adduct and a 1:2 adduct in which a bromo group has been displaced (eq 13).



The  $^{119}\text{Sn}$  NMR spectrum ( $-80$  °C,  $\text{CH}_2\text{Cl}_2$ ) of a 1:1 mixture of  $\text{Bu}_3\text{PO}$  and **5** shows a broad resonance at  $-89.3$  ppm, a doublet at  $-255.6$  ppm,  $^2J(^{119}\text{Sn}-^{31}\text{P}) = 160$  Hz, and a triplet at  $-326.3$  ppm,  $^2J(^{119}\text{Sn}-^{31}\text{P}) = 244$  Hz, all of approximately equal intensity. When the ratio of  $\text{Bu}_3\text{PO}$  is increased to 2:1, only the triplet at  $-326.3$  ppm remains, with further addition of  $\text{Bu}_3\text{PO}$  (4:1) not affecting the spectrum. No  $^{119}\text{Sn}$  NMR signals are observed at higher temperatures. These NMR data suggest that **5** undergoes halide displacement more readily than **4**. Thus, the three signals observed for the 1:1 mixture of **5** and  $\text{Bu}_3\text{PO}$  result from  $\text{PhI}_2\text{SnL}$  (**5**),  $\text{PhI}_2\text{SnL} \cdot \text{Bu}_3\text{PO}$ , and  $[\text{PhISnL} \cdot 2\text{Bu}_3\text{PO}]^+\text{I}^-$ , respectively. The addition of additional mole equivalents of  $\text{Bu}_3\text{PO}$  results in the exclusive formation of  $[\text{PhISnL} \cdot 2\text{Bu}_3\text{PO}]^+\text{I}^-$ .

These studies show that in the presence of a strong intermolecular donor, the tin atoms in compounds **3**–**5** do not become six-coordinate. Instead, the added Lewis base competes with the halide substituents for a coordination site, compound **5** showing the least resistance to halide displacement. It is well-known that diorganotin dihalides can form six-coordinate tin products through intermolecular or intramolecular coordination.<sup>26</sup> Consequently, the inability of compounds **3**–**5** to attain six-coordination through the interaction of an intermolecular donor results from steric restraints imposed around the tin atoms by the bulky ligand, L.

The almost temperature independent  $^{119}\text{Sn}$  NMR chemical shift (Table 3) of  $\text{Ph}(\text{SPh})_2\text{SnL}$ , **6**, in solution is very close to its solid state isotropic  $^{119}\text{Sn}$  chemical shift,  $\delta_{\text{iso}}$  28 ppm, indicating very similar structures in solution and in the solid state. Thus, the tin atom in **6** has a distorted tetrahedral configuration.

The  $^{119}\text{Sn}$  NMR (toluene) spectrum of **7**,  $\text{Cl}_3\text{SnL}$ , at  $100$  °C shows one resonance at  $-159.0$  ppm. At  $25$  °C, no  $^{119}\text{Sn}$  NMR ( $\text{CH}_2\text{Cl}_2$ ) resonance is observed, but upon cooling to  $-25$  °C a low intensity resonance is observed at  $-158.7$  ppm along with a major signal at  $-198.2$  ppm (ratio 1:15, respectively). The  $^{119}\text{Sn}$  NMR spectrum at

**Table 4.**  $^{119}\text{Sn}$  NMR ( $\text{CH}_2\text{Cl}_2$ ) Data for Compounds 9–13

compd	T, °C	$\delta(^{119}\text{Sn})$ , ppm	compd	T, °C	$\delta(^{119}\text{Sn})$ , ppm
<b>9</b>	+25	-109.8	<b>12</b>	+25	-163.3
	-80	-105.3		-55	-141.2
<b>10</b>	+25	-4.7	<b>13</b>	-80	-133.7
	-55	-31.4		+25	-107.2
	-80	-40.7		-55	-142.6
<b>11</b>	25	-26.4	-80	-154.3	
	-55	-53.0			
	-80	-64.0			

$-80$  °C shows only one signal ( $-205.3$  ppm). At  $25$  °C, the  $^1\text{H}$  and  $^{13}\text{C}$  NMR spectra of **7** show one resonance for the respective homologous ligand phenyl group substituents. At low temperature, they split into two resonances of equal intensity.

Compound **7** appears also to exhibit coordination equilibria with the equilibrium favoring almost exclusively the five-coordinate tin species as a result of the higher Lewis acidity of the  $\text{SnCl}_3$  fragment. The low-intensity  $^{119}\text{Sn}$  NMR signal at  $-25$  °C ( $-159.7$  ppm) is assigned to the four-coordinate species, while the major signal at  $-198.2$  ppm is assigned to the five-coordinate tin species. Lowering the temperature causes the  $^{119}\text{Sn}$  NMR resonance of the four-coordinate species to broaden, leaving only the resonance corresponding to the five-coordinate species. The isotropic  $^{119}\text{Sn}$  NMR chemical shift of  $\delta_{\text{iso}}$   $-176$  ppm in the solid state is in agreement with pentacoordination.

Both the  $^1\text{H}$  and  $^{13}\text{C}$  NMR spectra of **7** indicate that only the five-coordinate species is present at low temperature. The  $^2J(^{119}\text{Sn}-^1\text{H})$  and  $^1J(^{119}\text{Sn}-^{13}\text{C})$  couplings of 132 and 897 Hz observed at low temperature are quite large compared to those for compounds **4** and **5** but are still within the expected range for five-coordinate tin species of this class.<sup>27</sup>

In order to assess whether ring size affected the ability of the methoxy groups to participate in intramolecular coordination to tin, complexes based on  $\text{LCH}_2\text{-Br}$ , **8**, were synthesised. This second ligand system allows evaluation of any differences, which might be due to ring size, i.e., five-membered rings with L and six-membered rings with ( $\text{LCH}_2\text{H}$ ).

The almost temperature-independent  $^{119}\text{Sn}$  NMR chemical shift,  $-109.8$  ppm (Table 4), and  $^1J(^{119}\text{Sn}-^{13}\text{CH}_2)$  constant of 377 Hz indicate that the tin atom in **9** is four coordinate. At room temperature, the  $^1\text{H}$  and  $^{13}\text{C}$  NMR data of **9** show equivalence of the homologous ligand phenyl group substituents. However, unlike **1**, these signals only become broad at low temperature and are not split. These results suggest that rotation of the substituted ligand phenyl rings in **9** is less hindered compared with those in **1**.

The room-temperature  $^1\text{H}$  and  $^{13}\text{C}$  NMR data for compounds  $\text{PhCl}_2\text{Sn}(\text{CH}_2\text{L})$  (**10**),  $\text{PhBr}_2\text{Sn}(\text{CH}_2\text{L})$ , (**11**),  $\text{PhI}_2\text{Sn}(\text{CH}_2\text{L})$  (**12**), and  $\text{Cl}_3\text{Sn}(\text{CH}_2\text{L})$  (**13**) show equivalence of the respective homologous ligand phenyl group substituents. At low temperature, compounds **10**–**12** exhibit broad resonances in the  $^1\text{H}$  NMR ( $\text{CD}_2\text{Cl}_2$ ,  $-110$  °C) spectra, whereas the spectrum of **13** shows two peaks for  $\text{C}(\text{CH}_3)_3$  (1.24, 1.35 ppm), Me (2.12, 2.27 ppm), and OMe (3.19, 4.14 ppm). Broad peaks are observed for the  $\text{CH}_2$  (no couplings visible), CH, and aromatic

(25) Colton, R.; Dakternieks, D. *Inorg. Chim. Acta.* **1988**, *148*, 31.  
 (26) (a) Schollmeyer, D.; Hartung, H.; Klaus, C.; Jurkschat, K. *Main Group Metal Chem.* **1991**, *14*, 27 and references cited therein. (b) Van Koten, G.; Jastrzebski, J. T. B. H. *J. Organomet. Chem.* **1979**, *177*, 283. (c) Harrison, P. G.; King, T. J.; Healy, M. A. *J. Organomet. Chem.* **1979**, *182*, 17. (d) Hartung, H.; Krug, A.; Richter, F.; Weichmann, H. *Z. Anorg. Allg. Chem.* **1993**, *619*, 859. (e) Van Koten, G.; Jastrzebski, J. T. B. H. *Advances Organomet. Chem.* **1993**, *35*, 241 and references cited therein.

(27) Fouquet, E.; Jousseau, B.; Maillard, B.; and Perere, M. *J. Organomet. Chem.* **1993**, *453*, C1.

moieties (2.84, 4.93, and 6.82–7.24 ppm, respectively). The resonances observed in the low-temperature  $^{13}\text{C}$  NMR ( $\text{CDCl}_2$ ,  $-80\text{ }^\circ\text{C}$ ) spectra of compounds **10**–**13** are all broad.

Compounds **10**, **11**, and **13** show a progressive shift to low frequency of their  $^{119}\text{Sn}$  NMR signals with a decrease in temperature (Table 4). As was the case for  $\text{PhI}_2\text{SnL}$ , the behavior of  $\text{PhI}_2\text{Sn}(\text{CH}_2\text{L})$  appears anomalous, with a progressive shift to higher frequency of its  $^{119}\text{Sn}$  NMR signal with a decrease in temperature.

The NMR data for compounds **10**–**13** are explained in terms of temperature-dependent equilibria between four- and five-coordinate species. Unlike the five-membered ring analogues **3**, **4**, and **7**, the equilibria involving compounds containing six-membered rings are fast on the NMR time scale at all temperatures measured and only averaged signals are observed. The tin centers in the six-membered ring compounds are expected to have almost the same Lewis acidity as those in the five-membered ring systems **3**–**5** and **7**. Consequently, the greater rate constants for the equilibria involving **10**–**13** result from greater lability imparted by the larger ring size in these compounds **16**.<sup>26e</sup> The population of four- and five-coordinate species for **10**, **11**, and **13** is temperature dependent, with the higher coordination again being favored at low temperature. The equilibrium for **12** lies almost exclusively toward four-coordinate tin.

## Conclusion

The ability of intramolecular coordination to take place in the two series of compounds **1**, **3**–**7** and **9**–**13** depends both on the Lewis acidity at tin and the ring size formed on intramolecular coordination. The Lewis acidity is controlled by the nature of the ligands (in addition to L or  $\text{CH}_2\text{L}$ ) attached to tin. The six-membered rings in the series containing  $\text{CH}_2\text{L}$  are more labile than the five-membered rings possible in the series containing L. In neither series (L or  $\text{CH}_2\text{L}$ ) was there any evidence for intramolecular coordination of both methoxy groups to tin and neither L nor  $\text{CH}_2\text{L}$  are suitable for synthesis of octahedral organotin trihalides with a facial arrangement of halides.

**Acknowledgment.** We are grateful to the Australian Research Council (ARC) and the Stifterverband für die Deutsche Wissenschaft for financial support and to the Commonwealth of Australia for a Postgraduate Research Scholarship (R.T.).

**Supporting Information Available:** Tables of anisotropic thermal parameters, hydrogen atom parameters, bond distances, and bond angles for  $[\text{Ph}_3\text{SnL}]$ ,  $[\text{Ph}_3\text{SiL}]$ ,  $[\text{PhSnCl}_2\text{L}]$ ,  $[\text{PhSnBr}_2\text{L}]$ ,  $[\text{PhSnI}_2\text{L}]$ , and  $[\text{PhSn}(\text{SPh})_2\text{L}]$  (34 pages). Ordering information is given on any current masthead page.

OM960956B